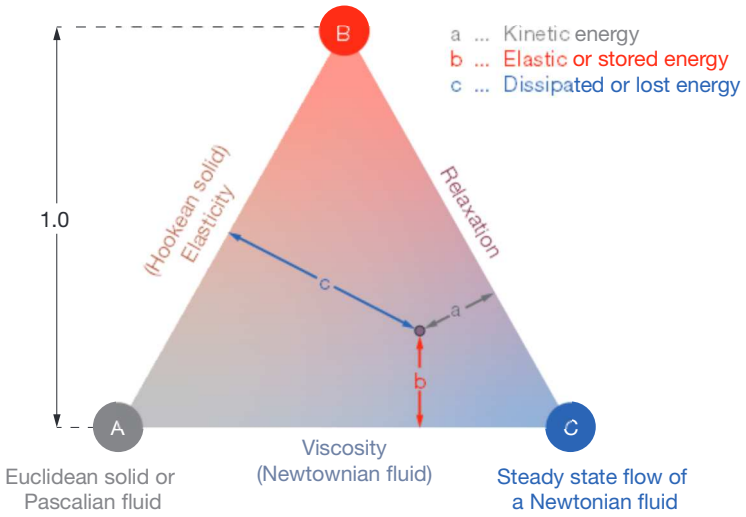

Figure 1.3 Rheological energy in triangular coordinates

1.2 Viscous Liquids or the Newtonian Fluid

Sir Isaac Newton (Fig. 1.4) was the first person to formulate a hypothesis that described the resistance to motion experienced by deforming fluids. In 1686 he published this work in Philosophiæ Naturalis Principia Mathematica [4] in a chapter titled "On the Circular Motion of Liquids". His hypothesis clearly states what we know today as a characterictic of a Newtonian fluid[2]:

That the resistance which arises from the lack of slipperiness of the parts of the fluid, other things being equal, is proportional to the velocity with which the parts of the liquid are separated from one another.

The phenomenon, described by Newton as "*defectu lubricitatis*," or "lack of slipperiness" between two fluid particles, was attributed to "*attritus*," meaning internal friction, or viscous friction. Since that time, the term "internal friction" and "viscous friction" have been used interchangeably. Although Newton's original work contains a mistake, corrected by Sir George Stokes [3] 150 years later, his main conclusion is still correct; it basically states that the force F required to maintain the motion between two fluid planes located at two arbitrary positions, say C and D in Newton's diagram (Fig. 1.5), is proportional to the difference between the velocity, u, of the

[2] The authors are using Emil Hatschek's translation from the Latin [2].

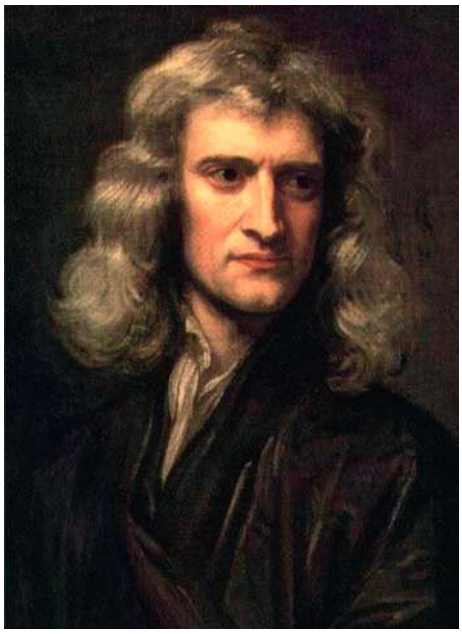

Figure 1.4
Sir Isaac Newton (1643–1727), painted in 1689 by Sir Godfrey Kneller

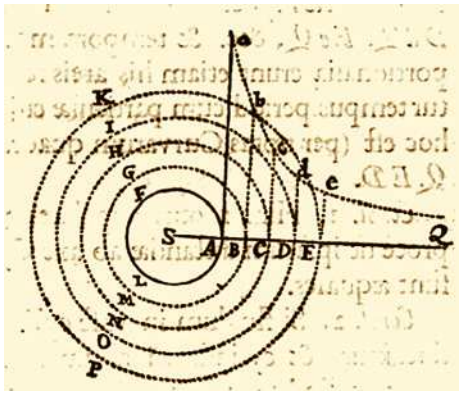

Figure 1.5
Diagram from Newton's 1686 publication [2]

two planes, and inversely proportional to the distance, r, between those two surfaces, the viscosity, η, and the area of the surfaces that separates them, A,[3]

$$F = A\eta \frac{u_\mathrm{d} - u_\mathrm{c}}{r_\mathrm{D} - r_\mathrm{C}} \tag{1.2}$$

[3] Newton used upper case A, B, C, D, etc. to describe the position of the surfaces, and lower case a, b, c, d, etc. to describe the velocity of those surfaces.

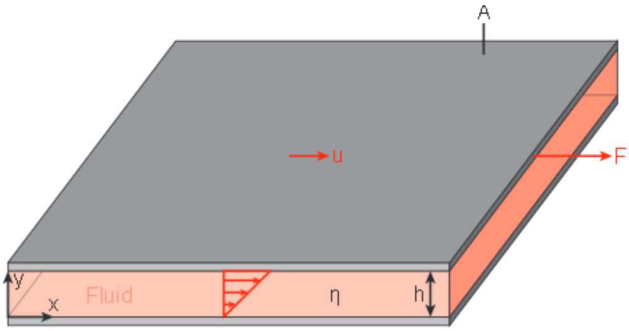

Figure 1.6 Simple shear flow with Cartesian coordinates

As shown in Newton's diagram, his analysis pertained to a rotating cylinder immersed in an infinitely large fluid body. For a more simplified system, such as the simple shear flow generated between two parallel plates presented in Fig. 1.6, Equation 1.2 can be expressed in terms of shear stress, and written as

$$F/A = \eta \frac{u}{h} \tag{1.3}$$

or

$$\tau_{xy} = \eta \dot{\gamma}_{xy} \tag{1.4}$$

where τ_{xy} is the shear stress in the x direction on a plane with its normal direction pointing in the y direction, and $\dot{\gamma}_{xy}$ is the corresponding rate of shear, or rate of deformation. The stress (here τ_{xy}) that leads to the deformation of the fluid contained within the system is also often referred to as the deviatoric stress[4].

The Newtonian model, or the viscous component of a material, is often also represented using a dashpot, shown in Fig. 1.7.

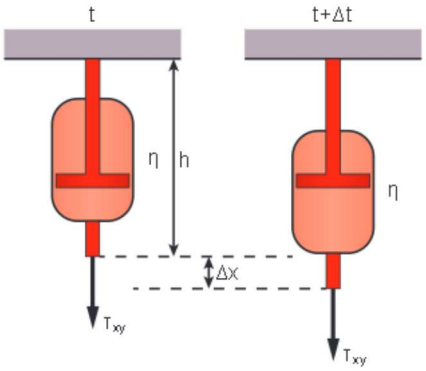

Figure 1.7 The dashpot – a schematic representation of a Newtonian fluid

[4] As will be shown in Chapter 2, which covers flow, the total stress, σ, is divided into the deviatoric stress component, τ, which causes deformation, and the hydrostatic stress component, which results from pressure, p.

While the schematic representation in Fig. 1.7 reflects an elongational deformation along the *x*-axis, the dashpot can also be used for shear deformation, which is written as

$$\gamma_{xy} = \frac{\Delta x}{h} \tag{1.5}$$

Figure 1.7 also shows that the deformation is time dependent and, in the case of a Newtonian fluid, the dependence between deformation and time is linear. In terms of shear strain rate, we can write

$$\gamma_{xy} = \dot{\gamma}_{xy}\,\Delta t \tag{1.6}$$

In Fig. 1.8, the strain within a Newtonian fluid, labeled as viscous strain, is presented for the case where a constant stress is applied during a time period from 0 to Δt. Once the load is released at time Δt, the material element remains deformed. This reflects point "C" in the Eisenschitz, Rabinowitsch and Weissenberg triangle, at which all energy is dissipated or lost and the deformation can no longer be recovered.

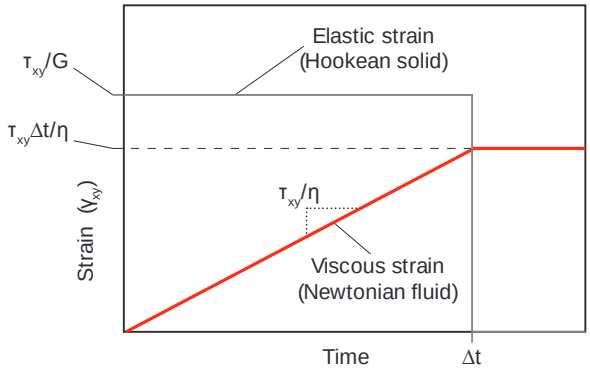

Figure 1.8 Strain response of a Newtonian fluid and a Hookean solid

1.3 Linear Elasticity or the Hookean Spring

Robert Hooke is a relatively unknown English scientist and engineer of the 17th century, who was completely overshadowed by his contemporary, Isaac Newton. In fact, an animosity between the two existed after Hooke claimed that Newton's work on gravitation was based on work he had done. As a result, Newton's obsession was to make sure that Hooke be forgotten; something he almost accomplished. Two years after Hooke's death in 1703, Newton became president of the Royal Society, and in that function made sure that every memory of Hooke was erased from the society, including his portrait and laboratory equipment, which mysteriously disappeared when the Royal Society moved to a new location after 1705.

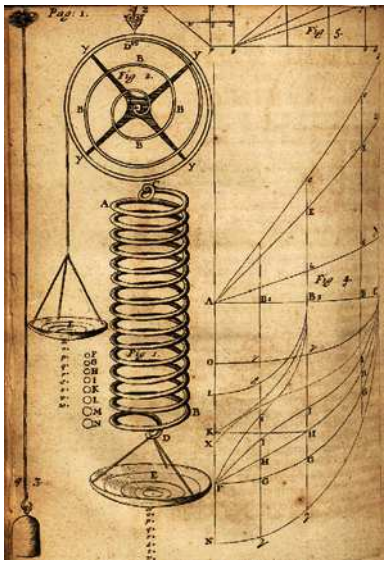

Figure 1.9 Diagram from Hooke's 1678 paper

However, while Hooke is certainly not part of popular culture in the way Newton has become, today his name remains well known among engineers who deal with solid mechanics, thanks to his theory of linear elasticity. Robert Hooke was the first person to find a relation between force and deflection in linear elastic solids, and published that work in his 1678's "*Lectures de Potentia Restitutiva*," or, "Of Spring". The basic theory behind what we today refer to as the Hookean spring (Fig. 1.9) is summarized in Latin by Hooke's words "*Ut tension sic vis*" or "*As the extension, so the force*." More simply stated, we can say that the force, F, is directly proportional to the deflection, Δx. This can be written using

$$F = k\,\Delta x \tag{1.7}$$

where k is the constant of proportionality or the spring constant, also called the stiffness. Hooke's concept was modified in 1727 by Leonhard Euler, who represented the force in terms of stress, F/A, and the displacement in terms of strain, $\Delta x/h$, where h represents the original length. The units in the constant of proportionality can be adjusted by using a modulus of elasticity or stiffness, E, or for a system that is deformed in shear, such as the one depicted in Fig. 1.10, a modulus of rigidity, G,

$$F/A = G\left(\Delta x/h\right) \tag{1.8}$$

In terms of stress and strain the above equation can be written as

$$\tau_{xy} = G\gamma_{xy} \tag{1.9}$$

where τ_{xy} is the shear stress and γ_{xy} the corresponding shear strain.

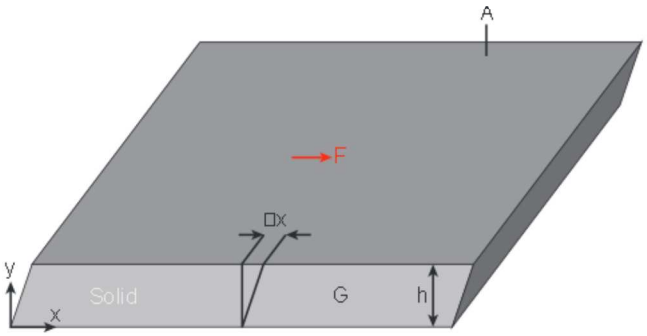

Figure 1.10 Perfectly Hookean solid deformed in shear

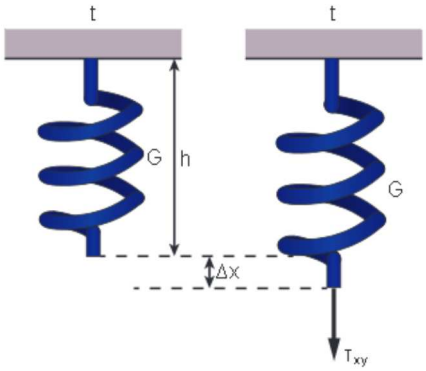

Figure 1.11 The spring – a schematic representation of a Hookean solid

Just like Hooke's approach in 1678, today the elastic component of a material is often represented using a spring, as shown in Fig. 1.11. The spring reflects a stretching body; however, it can also be used to represent shear. In Fig. 1.11 we can see how the spring deforms as soon as the load is applied and remains constant as long as the load remains the same. Once the load is released at time D*t*, the material element will almost instantly return to its initial shape. This reflects point "B" in the Eisenschitz, Rabinowitsch and Weissenberg triangle, where the energy is stored and fully recovered.

In his publication, Robert Hooke boldly concluded that the elastic behavior is not only observed in springs, "but in all other springy bodies whatsoever, whether Metal, Wood, Stones, baked Earths, Hair, Horns, Silk, Bones, Sinews, Glass, and the like." His statement may be true for metal, stone, baked earths, and perhaps glass; however, all the other materials have a viscous force component, introducing time dependency when they are deformed, and should therefore be considered as viscoelastic materials.

1.4 Viscoelasticity and the Maxwell Model

After Newton and Hooke proposed their fluid and solid models, the world would have to wait almost two centuries before someone would attempt to model the behavior of a body that has both a viscous and an elastic force component during deformation. In 1867, James Clerk Maxwell (Fig. 1.12) published his paper "On the Dynamical Theory of Gases" [16], in which he presented a model for a system that combines elastic and viscous effects. His model and the resulting linear differential equations that relate stress and strain represent today's Maxwell model, which is graphically depicted by an instantaneous change of the spring and a time-dependent reaction, $t + \Delta t$, of the dash-pot in series, as depicted in Fig. 1.13.

In principle, the model is based on the fact that when a stress τ_{xy} is applied to the system, this stress is the same in both fluid and solid elements, and the total strain is the sum of the elastic strain, γ^{G}_{xy}, and the viscous strain, γ^{η}_{xy}, such that

$$\tau_{xy} = \tau^{\eta}_{xy} = \tau^{G}_{xy} \tag{1.10}$$

and

$$\gamma_{xy} = \gamma^{G}_{xy} + \gamma^{\eta}_{xy} \tag{1.11}$$

which can also be differentiated in time to give a function for total rate of deformation, or rate of strain

$$\dot{\gamma}_{xy} = \dot{\gamma}^{G}_{xy} + \dot{\gamma}^{\eta}_{xy} \tag{1.12}$$

Figure 1.12
James Clerk Maxwell

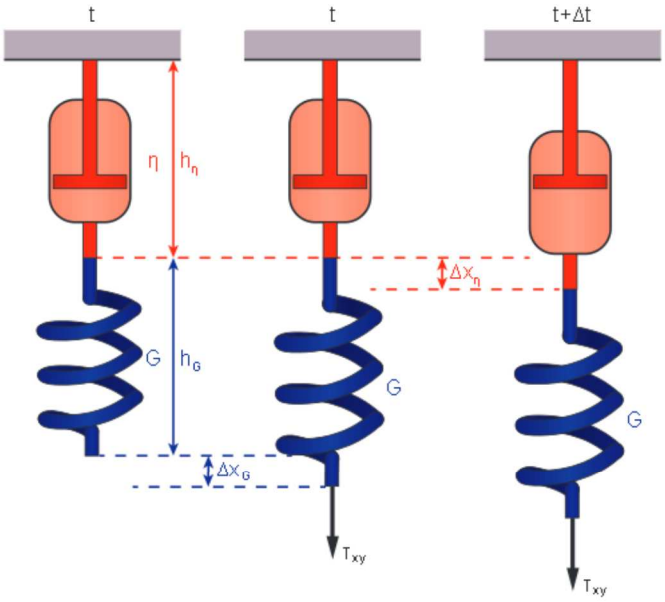

Figure 1.13 Schematic representation of the viscoelastic Maxwell model

Combining Eqs. 1.10–1.12 with the constitutive laws for the dash-pot (Eq. 1.4) and the spring (Eq. 1.9), results in Maxwell's linear differential equation given by

$$\frac{\mathrm{d}\tau_{xy}}{\mathrm{d}t} = G\frac{\mathrm{d}\gamma_{xy}}{\mathrm{d}t} - \frac{\tau_{xy}}{\lambda} \tag{1.13}$$

where $\lambda = G/\eta$, which Maxwell called "time of relaxation", and which is now commonly referred to as relaxation time.

In the case of constant stress, Maxwell's linear differential equation is solved for strain

$$\gamma_{xy} = \frac{\tau_{xy}}{\eta}t + \frac{\tau_{xy}}{G} \tag{1.14}$$

which is schematically shown in Fig. 1.14 for the case where the constant stress τ_{xy} is applied from $t = 0$ to $t = \Delta t$. The figure shows how the material element experiences an instant deflection, caused by its elastic component, and continues to deform at a constant rate, caused by its viscous component. The continuous flow experienced by the material under constant load is commonly referred to as creep or retardation. Once the load is released, the stored elastic deformation is recovered, and the viscous deformation remains.

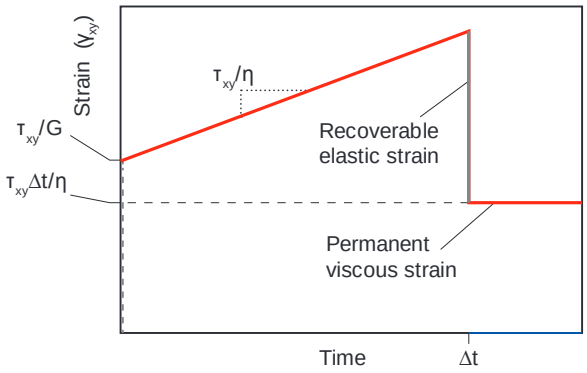

Figure 1.14 Creep in a Maxwell model

In the case of constant strain applied to the Maxwell material model, the linear differential equation is solved for stress

$$\tau_{xy} = G\gamma_{xy}\, e^{-\frac{t}{\lambda}} \tag{1.15}$$

which is schematically depicted in Fig. 1.15 for a case where G = 100 MPa, λ = 1 s and the imposed strain γ_{xy} = 1. Here, we see a gradual reduction in stress, a phenomenon commonly referred to as stress relaxation, which is represented by the line BC on the Eisenschitz, Rabinowitsch and Weissenberg triangle (see Fig. 1.3). At point B in their triangle, the relaxation time λ is infinite, reflecting a Hookean solid, while at position C it is zero, which reflects a Newtonian fluid.

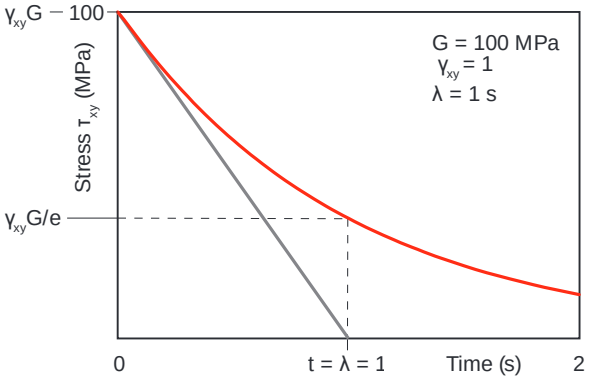

Figure 1.15 Stress relaxation in a Maxwell model

3.2.3 The Cross-WLF Model

This 6-parameter model considers the effects of shear rate and temperature on the viscosity. Similar to the Bird-Carreau model, this model describes both Newtonian and shear thinning behavior. The shear thinning part is modeled by the general Cross equation [12], which is a popular and earlier alternative to the Bird-Carreau-Yasuda model:

$$\frac{\eta_{\dot{\gamma}} - \eta_\infty}{\eta_0 - \eta_\infty} = \frac{1}{1 + \left(K \cdot \dot{\gamma}\right)^{1-n}} \tag{3.19}$$

where η_0 is the zero shear rate viscosity, η_∞ is an infinite shear rate viscosity, K is a time constant such as k_2 in Table 3.5, and n is the Power Law index, which accounts for the shear thinning behavior. For $\eta_{\dot{\gamma}} \to \eta_0$ and $\eta_{\dot{\gamma}} \to \eta_\infty$, the Cross model reduces to the Power Law model. If the infinite shear rate viscosity is negligible, the well-known form of the Cross model can be written as

$$\eta\left(\dot{\gamma}\right) = \frac{\eta_0}{1 + \left(\frac{\eta_0 \dot{\gamma}}{\tau^*}\right)^{1-n}} \tag{3.20}$$

Here, τ^* is the critical shear stress at the transition from the Newtonian plateau, with $K = \eta_0 / \tau^*$, and n is the Power Law index, see Fig. 3.9. If the model is used to fit the data prior to making the Weissenberg-Rabinowitsch correction (see Eq. 6.19 in Chapter 6), the apparent shear stress can be shifted [13] by setting

$$\tau^* = \left(\frac{4n}{3n+1}\right)^{\frac{n}{1-n}} \tag{3.21}$$

In this case, the remaining model parameters remain unchanged.

The zero shear viscosity is modeled with the WLF equation

$$\eta_0\left(T\right) = D_1 \cdot \exp\left[\frac{A_1\left(T - D_2\right)}{A_2 + T - D_2}\right] \tag{3.22}$$

where D_1 is the viscosity at a reference temperature D_2 and A_1 and A_2 describe the temperature dependency, which is comparable to the temperature shift factor described in Eq. 3.9.

The Cross-WLF model is the most common model used by injection molding simulation software, because it offers the best fit to most viscosity data [14]. Table 3.6 presents constants for various common thermoplastics.

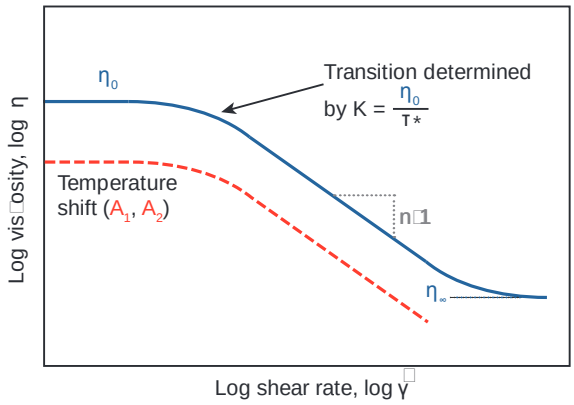

Figure 3.9 Viscosity approximation with the Cross-WLF model in Eq. 3.20 and Eq. 3.22

Table 3.6 Constants for the Cross-WLF Model for Various Common Thermoplastics [15, 16]

Polymer	τ (Pa)	n	D_1 (Pa s)	D_2 (K)	A_1	A_2 (K)
Polystyrene	31,200	0.243	1223	503	6.5	158.2
High density polyethylene	75,700	0.342	7×10^{12}	153	26.3	51.6
Low density polyethylene	34,515	0.315	3.1×10^{14}	233	34.6	51.6
Polypropylene	32,477	0.251	564	493	2803.3	165,097.1
Polyamide 66	151,905	0.347	144	573	256,999.6	11,235,949
Polycarbonate	8,437,056	0.116	462	573	8.4	246.8
Polyvinyl chloride	46,070	0.399	3.2×10^{16}	353	42.9	51.6

3.2.4 The Bingham Model

The Bingham model is an empirical two-parameter model that represents the rheological behavior of materials that exhibit yield stresses τ_0, below which the material does not flow. Typical examples of Bingham fluids are polymer emulsions and slurries. In the flow range, above the yield stress, a Bingham fluid behaves like a Newtonian liquid and can therefore be represented as

$$\eta = \infty \quad \text{or} \quad \dot{\gamma} = 0 \quad \text{for} \quad \tau \le \tau_0 \tag{3.23}$$

$$\eta = \mu_0 + \frac{\tau_0}{\dot{\gamma}} \quad \text{for} \quad \tau > \tau_0 \tag{3.24}$$

Here, τ is the magnitude of the deviatoric stress tensor and μ_0 is the Newtonian viscosity for vanishing yield stress. The model shows that a critical level of stress must be attained in order to initiate flow.

3.2.5 The Herschel-Bulkley Model

The Herschel-Bulkley model is widely used to represent the behavior of fluids that have a yield stress, such as the Bingham fluid, but that otherwise exhibit shear thinning behavior. The model is represented as

$$\tau = \tau_0 + m \cdot \dot{\gamma}^n \tag{3.25}$$

$$\eta = \frac{\tau_0}{\dot{\gamma}} + m \cdot \dot{\gamma}^{n-1} \quad \text{for} \quad \tau > \tau_0 \tag{3.26}$$

where τ_0 is the yield stress, m the consistency index, and n the Power Law or flow index. As with the Bingham model, this model also requires that a critical level of stress must be attained to initiate flow. Below this critical stress τ_0, the material behaves like a solid, allowing it to sustain stress without flow, but above the critical stress, the material flows like a Power Law fluid. Similar to the Power Law model, $n < 1$ represents shear thinning, $n > 1$ shear thickening, and $n = 1$ reduces the model to the Bingham model and represents Newtonian flow above the critical yield stress.

Table 3.7 shows that all models discussed so far can be derived from one base equation. While the Power Law model is the simplest model that can be used when the shear rate is high, the Cross-WLF model is the most common model in numerical simulations because it fits the viscosity data of a wide range of materials. In terms of practical applications, it is closely followed by the Bird-Carreau-Yasuda model.

Table 3.7 Overview of Viscous Flow Models

	Power Law	Bird-Carreau-Yasuda	Cross-WLF	Bingham
Base equation	$\frac{\eta-\eta_\infty}{\eta_0-\eta_\infty} = \frac{1}{\left[1+(K\dot{\gamma})^a\right]^{\frac{(1-n)}{a}}}$			
Assumptions	$\eta \ll \eta_0$, $\eta \gg \eta_\infty$, $\eta_\infty = 0$, $a = 1$, $K = m$	$\eta_\infty = 0$, $K = \lambda$	$\eta_\infty = 0$, $a = 1$, $K = \frac{\eta_0}{\tau^*}$	$\eta \ll \eta_0$, $\eta \gg \mu_0$, $K = \tau_Y$, $n = 0$
Model	$\eta = m \cdot \dot{\gamma}^{n-1}$	$\eta = \frac{\eta_0}{\left(1+\lvert\lambda\dot{\gamma}\rvert^a\right)^{\frac{(1-n)}{a}}}$	$\eta = \frac{\eta_0}{1+\left(\frac{\eta_0\dot{\gamma}}{\tau^*}\right)^{1-n}}$	$\eta = \mu_0 + \frac{\tau_Y}{\dot{\gamma}}$

5 Viscoelasticity

Although polymers have their distinct transitions and may be considered liquid when above the glass transition or melting temperatures, or solid when below those temperatures, in reality they are neither liquid nor solid, but viscoelastic. In fact, at any temperature, a polymer can be either a liquid or a solid, depending on the time scale or the speed at which its molecules are being deformed.

We can use the Deborah number, $De = \lambda\,\omega$, first discussed in Chapter 1, and the deformation, γ_0, to summarize how the system can be most accurately modeled. Figure 5.1 helps visualize the relation between time scale, deformation, and applicable material behavior. At small Deborah numbers, the polymer can be modeled as a Newtonian fluid, and at very high Deborah numbers, the material can be modeled as a Hookean solid. Both cases are well understood; the first is extensively covered in Chapters 3 and 4, and the latter within the field of solids mechanics, outside the scope of this book.

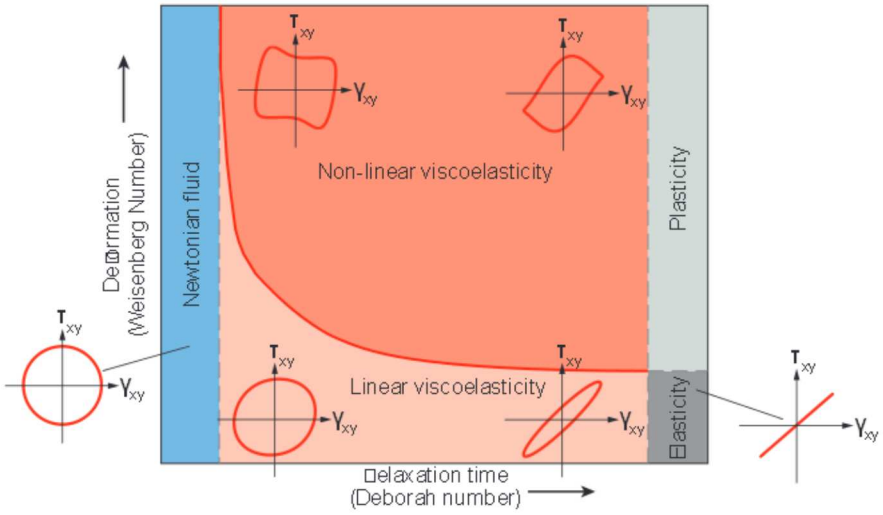

Figure 5.1 Schematic of Newtonian, elastic, linear, and non-linear viscoelastic regimes as a function of deformation and relaxation time during deformation of polymeric materials

The cases that fall between these two situations are covered within this chapter. Here, the viscoelastic region is divided in two: the linear viscoelastic region for small deformations, and the non-linear viscoelastic region for large deformations.

Experimentally, simple laboratory tests are desirable in order to obtain information relevant to actual processing conditions. Experiments that apply small deformations are used to study linear viscoelasticity, revealing information about the molecular structure. Here, the material functions and models are useful for predicting general tendencies and for quality control in production. A comprehensive guide to understanding linear viscoelasticity is given by Ferry [1]. For actual processing-relevant information, however, the more complex, viscoelastic behavior under large deformations must be studied, typically using large amplitude oscillatory shear (LAOS) tests.

The collected data can be displayed in the form of Lissajous loops or they can be presented on a so-called Pipkin diagram, where instead of deformation, the Weissenberg number, $We = \gamma_0 \lambda \omega$, is on the vertical axis

5.1 Linear Viscoelasticity

The well-established field of linear viscoelasticity applies to materials undergoing small deformations, such as the short term deformation of polymer components. The most common, linear viscoelastic model is the Maxwell model presented in Chapter 1. The governing equation for the Maxwell model is given by

$$\tau_{xy} + \lambda \frac{\mathrm{d}\tau_{xy}}{\mathrm{d}t} = -\eta_0 \dot{\gamma}_{xy} \tag{5.1}$$

Experimentally, linear viscoelasticity is maintained during a dynamic mechanical test (DMA) or oscillatory sliding plate rheometry, where the small deformations leave the molecular structure almost unaffected and the same response is observed in each cycle during testing. The non-linearities arise as soon as the deformation is large enough to alter the structure of the polymer chains. This, of course, is the topic for non-linear viscoelasticity discussed later in this chapter.

5.1.1 Relaxation Modulus

As discussed in Chapter 2, the most basic principle that governs the mechanical and rheological behavior of polymers is the stress relaxation behavior. When a sudden strain is applied at $t = 0$, such as a small amount of shear γ_0, the resulting

stress can be measured as a function of time, $\tau(t)$. For non-linear materials, such as polymers, the decaying stress results in a shear modulus that is also a function of strain $G(\gamma_0, t)$, where

$$G(\gamma_0, t) = \tau_{xy}(\gamma_0, t)/\gamma_0 \tag{5.2}$$

Similar to the stress relaxation modulus presented for elongational deformations in Chapter 2, we can assume that for small instantaneous deformations the shear modulus is proportional to strain and is therefore only a function of time

$$G(t) = \tau_{xy}(t)/\gamma_0 \tag{5.3}$$

This linear relation is the basic principle behind linear viscoelasticity.

5.1.2 The Boltzmann Superposition Principle

In addition to the *time-temperature superposition principle (WLF)*, the *Boltzmann superposition principle* is of extreme importance in the theory of linear viscoelasticity. The Boltzmann superposition principle states that the deformation of a polymer component is the sum or superposition of all strains that result from various loads acting on the part at different times. This means that the response of a material to a specific load is independent of already existing loads or strains. That is, if at a particular time t_i a sudden strain $\Delta\gamma(t_i)$ is applied, the resulting stress from this strain can be expressed as

$$\tau_{xy_i}(t) = G(t - t_i)\,\Delta\gamma_{xy_i}(t_i) \tag{5.4}$$

Hence, we can compute the stress within a polymer specimen that is exposed to several strains at different points in time (such as presented in Fig. 5.2) by simply adding all stress responses:

$$\tau_{xy}(t) = G(t - t_1)\,\Delta\gamma_{xy_1}(t_1) + G(t - t_2)\,\Delta\gamma_{xy_2}(t_2) + G(t - t_3)\,\Delta\gamma_{xy_3}(t_3) + \ldots \tag{5.5}$$

or

$$\tau_{xy}(t) = \sum_{i=1}^{n} G(t - t_i)\,\Delta\gamma_{xy_i}(t_i) \tag{5.6}$$

where $t > t_n$. For very small strain intervals that lead to a continuous strain function we can write the above sum in integral form

$$\tau_{xy}(t) = \int_{-\infty}^{t} G(t - t')\,\mathrm{d}\gamma_{xy}(t') \tag{5.7}$$

which can be written in terms of strain rate as

$$\tau(t) = \int_{-\infty}^{t} G(t-t')\,\dot{\gamma}_{xy}(t')\,\mathrm{d}t' \tag{5.8}$$

which in turn can be written in terms of compliance

$$\tau_{xy}(t) = \int_{-\infty}^{t} J(t-t')\,\dot{\tau}_{xy}(t')\,\mathrm{d}t' \tag{5.9}$$

In the case that the polymer component is stress-free at $t = 0$, we can write

$$\tau_{xy}(t) = \int_{0}^{t} G(t-t')\,\dot{\gamma}_{xy}(t')\,\mathrm{d}t' \tag{5.10}$$

Which, for systems with complex three-dimensional stress and strain fields, can be written in tensor form as

$$\underline{\underline{\tau}}(t) = \int_{0}^{t} G(t-t')\,\dot{\underline{\underline{\gamma}}}(t')\,\mathrm{d}t' \tag{5.11}$$

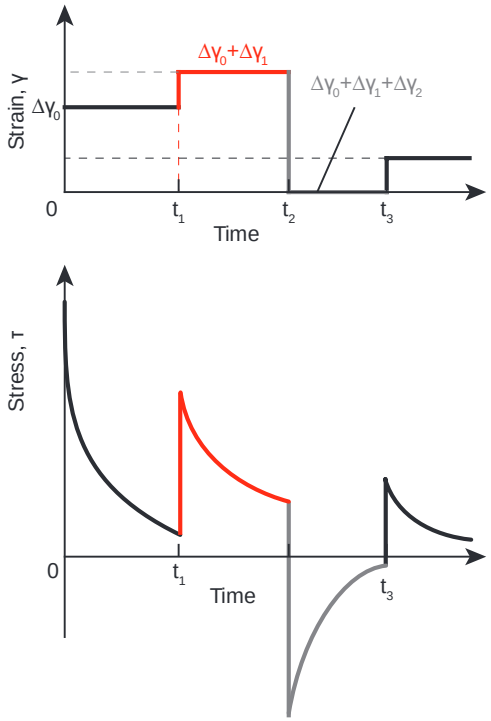

Figure 5.2 Schematic demonstration of Boltzmann's superposition principle

Table 6.1 Comparison between Cone-Plate and Parallel-Plate Rheometer

Property/setting	Cone-Plate	Parallel-Plate
Shear rate	**Constant shear rate in the conical gap**	Shear rate gradient from edge of plate to rotational axis; can be varied by adjusting the gap height H
Tests	All basic rheological tests such as tension, creep, relaxation, oscillation and ramp tests; variation of shear rate by adjustment of angular velocity Ω and cone angle θ	Simple variation of shear rate by adjustment of the angular velocity Ω and the gap height H
Normal stresses	Yes	Inaccurate
Materials/ suspensions	Measurement of polymer melts, but particle size is limited (≤ 10 µm), no solids	Measurement of materials with big particles as well as materials with 3D-structures; soft solids (special case: plastic melts at the transition to the solid), curing materials, filled polymer melts, elastomers, powders, and gels
Preload	Smaller preload requires shorter equilibration times	
Temperature range	The effect of thermal expansion or shrinkage is dependent on the gap height	
	e.g., DH = 5 µm, for H = 50 µm the change in viscosity measurement is 10%	e.g., DH = 5 µm, for H = 1 mm the change in viscosity measurement is only 0.5%

6.4 The Capillary Rheometer

The most common and simplest device for measuring shear rate viscosity in the processing range is the capillary rheometer. Its main component is a straight tube or capillary, and it was first used to measure the viscosity of water by Hagen [7] and Poiseuille [8]. A capillary rheometer has a pressure driven flow for which the velocity gradient or strain rate, and also the shear rate, will be maximum at the wall and zero at the center of the capillary, making the flow non-homogeneous.

Because pressure driven rheometers employ non-homogeneous flows, they can only measure steady shear functions, such as viscosity, $\eta(\bar{\dot{\gamma}})$. However, they are widely used because they are relatively inexpensive to build and simple to operate. Despite their simplicity, long capillary rheometers provide the most accurate and process relevant viscosity data available. Another major advantage is that capillary rheometers have no free surfaces in the test region, unlike other types of rheometers such as the cone-plate rheometers. When measuring the strain rate dependent viscosity of polymer melts, capillary rheometers may offer the only satisfactory method of obtaining such data at shear rates > 100 s^{-1}. This is important for processes with

higher rates of deformation, such as mixing, extrusion, and injection molding. Because their design is basic and they only need a pressure head at the entrance, capillary rheometers can easily be attached to the end of a screw- or ram-type extruder for online measurements. This makes the capillary rheometer an efficient tool for industry. The shear rate range is limited to shear rates above 1 s^{-1}, because below this rate the effects of surface tension, gravity, and friction between piston and reservoir are noticeable and must be included in the analysis. Measurements in this region lead to an overprediction of viscosity [9]. The upper shear rate limit is approx. 10^7 s^{-1}, or as soon as melt fracture occurs. Furthermore, viscous dissipation may become significant at those high shear rates.

The basic features of capillary rheometers are shown in Figure 6.6. A capillary tube of radius R and length L is connected to the bottom of a reservoir. The pressure drop and flow rate through this tube are measured at constant temperatures to determine the viscosity.

Standard ISO 11443 [10] defines two possible methods: either measuring the volume flow rate Q or the test pressure p, while keeping the other parameter constant. It is recommended to use capillaries with a length l of either 16 mm or 20 mm and a diameter of 1 mm. For highly filled materials, the diameter may be changed within certain specifications.

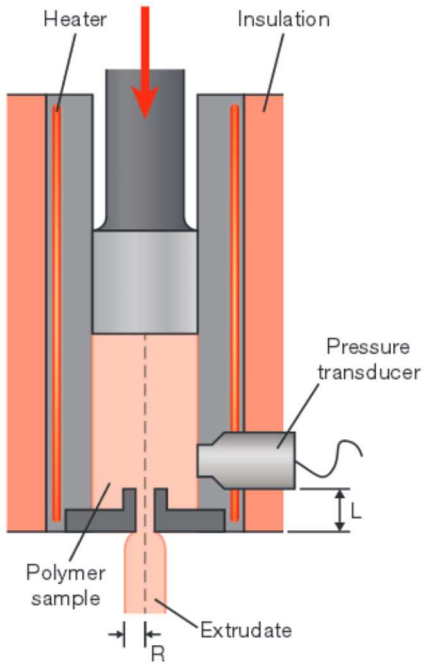

Figure 6.6 Schematic diagram of a capillary viscometer

To derive the viscosity relation, the following assumptions are made:

- no velocity in the radial, r, and the angular, θ, directions of the capillary,
- the polymer is incompressible, and
- flow is fully developed, steady, isothermal, and laminar.

The capillary rheometer can be modeled using the z-component of the equation of motion in terms of stress, τ, as

$$0 = \frac{\mathrm{d}p}{\mathrm{d}z} + \frac{1}{r}\frac{\mathrm{d}}{\mathrm{d}r}\left(r\tau_{rz}\right) \tag{6.12}$$

where

$$\frac{\mathrm{d}p}{\mathrm{d}z} = \frac{p_0 - p_\mathrm{L}}{L} \tag{6.13}$$

Integrating for the shear stress term gives:

$$\tau_{rz} = \frac{\left(p_0 - p_L\right)r}{2L} + \frac{C_1}{r} \tag{6.14}$$

The constant C_1 is assumed to be zero because the stress cannot be infinite at the tube axis.

6.4.1 Computing Viscosity Using the Bagley and Weissenberg-Rabinowitsch Equations

When computing viscosity from data measured using a capillary rheometer, the shear stress at the wall of the capillary must be corrected as proposed by Bagley because of entrance effects [11]. Furthermore, because the shape of the velocity profile is affected by the shear thinning behavior of the polymer, the shear rate at the wall is computed using the Weissenberg-Rabinowitsch correction [12].

At the wall the apparent shear stress is given by

$$\tau_{r=R} = \tau_\mathrm{aw} = \frac{R}{2}\frac{\left(p_0 - p_\mathrm{L}\right)}{L} = \frac{R}{2}\frac{\Delta p}{L} \tag{6.15}$$

Equation 6.15 requires that the capillary be sufficiently long to assure fully developed flow that renders entrance effects insignificant. At the same time, capillaries should be short so that viscous dissipation does not have to be considered. Due to end effects, the actual pressure profile along the length of the capillary exhibits a curvature, which is a source of error that must be corrected. This is shown schematically in Figure 6.7 [6].

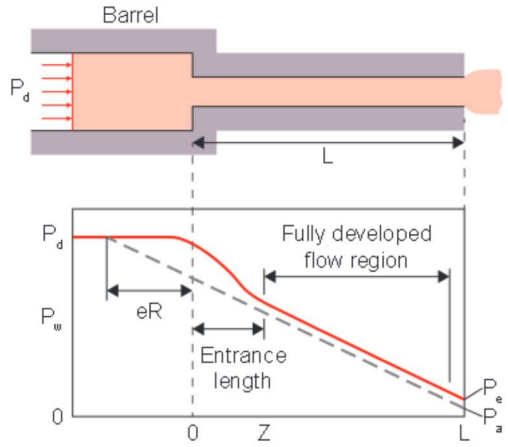

Figure 6.7 Entrance effects in a typical capillary rheometer

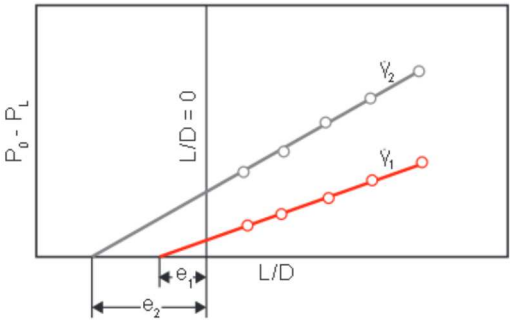

Figure 6.8 Bagley plots for two shear rates

For the correction, measurements with capillary dies of the same diameter and at least two different length-to-diameter ratios L/D must be performed. The correction factor e at a specific shear rate can be found by plotting the pressure drop for various capillary L/D ratios as shown in Figure 6.8 [6].

The true shear stress at the wall can now be calculated using the end correction e as,

$$\tau_w = \frac{1}{2}\frac{(p_0 - p_L)}{(L/D + e)} \tag{6.16}$$

The equation for shear stress can now be written as

$$\tau_{rz} = \frac{r}{R}\tau_w \tag{6.17}$$

The apparent or Newtonian shear rate $\dot{\gamma}_{aw}$ at the wall is

$$\dot{\gamma}_{aw} = \frac{4Q}{\pi R^3} \tag{6.18}$$

To obtain the true shear rate at the wall, du_z/dr, the Weissenberg-Rabinowitsch equation [12] can be used

$$-\frac{du_z}{dr} = \dot{\gamma}_w = \frac{1}{4}\dot{\gamma}_{aw}\left[3 + \frac{d(\ln Q)}{d(\ln \tau)}\right] \tag{6.19}$$

In slit dies the apparent and true shear stress are calculated using

$$\tau_{aw} = \frac{H \cdot W}{2(H+W)}\frac{\Delta p}{L} \tag{6.20}$$

and

$$\tau_w = \frac{H \cdot W}{2(H+W)}\frac{(p_0 - p_L)}{L+e} \tag{6.21}$$

and the apparent and true shear rates are calculated by

$$\dot{\gamma}_{aw} = \frac{6Q}{W \cdot H^2} \tag{6.22}$$

$$\dot{\gamma}_w = \frac{1}{3}\dot{\gamma}_{aw}\left[2 + \frac{d(\ln Q)}{d(\ln \tau)}\right] \tag{6.23}$$

The viscosity for both capillary and slit dies can now be calculated using

$$\eta = \frac{\tau_w}{\dot{\gamma}_w} \tag{6.24}$$

Slit dies with flush mounted pressure transducers allow the direct measurement of the pressure drop along the flow length. Then the true shear stress is obtained by

$$\tau = \frac{H \cdot W}{2(H+W)}\frac{\Delta p}{\Delta L} \tag{6.25}$$

where H is the thickness and W the width of the slit, and $\Delta p/\Delta L$ is the longitudinal pressure gradient. Although entrance and exit effects can be neglected, for aspect ratios $H/W > 0.1$, corrections for corner effects need to be made.

Subject Index